Search for High Mass Top Quark Production in $p\bar{p}$ Collisions at $\sqrt{s} = 1.8$ TeV

S. Abachi,[12] B. Abbott,[32] M. Abolins,[22] B. S. Acharya,[38] I. Adam,[10] D. L. Adams,[33] M. Adams,[15] S. Ahn,[12] H. Aihara,[19] G. Álvarez,[16] G. A. Alves,[8] E. Amidi,[26] N. Amos,[21] E. W. Anderson,[17] S. H. Aronson,[3] R. Astur,[36] R. E. Avery,[28] A. Baden,[20] V. Balamurali,[29] J. Balderston,[14] B. Baldin,[12] J. Bantly,[4] J. F. Bartlett,[12] K. Bazizi,[7] T. Behnke,[36] J. Bendich,[19] S. B. Beri,[30] I. Bertram,[33] V. A. Bezzubov,[31] P. C. Bhat,[12] V. Bhatnagar,[30] M. Bhattacharjee,[11] A. Bischoff,[7] N. Biswas,[29] G. Blazey,[12] S. Blessing,[13] A. Boehnlein,[12] N. I. Bojko,[31] F. Borcherding,[12] J. Borders,[34] C. Boswell,[7] A. Brandt,[12] R. Brock,[22] A. Bross,[12] D. Buchholz,[28] V. S. Burtovoi,[31] J. M. Butler,[12] O. Callot,[36,*] D. Casey,[34] H. Castilla-Valdez,[9] D. Chakraborty,[36] S.-M. Chang,[26] S. V. Chekulaev,[31] L.-P. Chen,[19] W. Chen,[36] L. Chevalier,[35] S. Chopra,[30] B. C. Choudhary,[7] J. H. Christenson,[12] M. Chung,[15] D. Claes,[36] A. R. Clark,[19] W. G. Cobau,[20] J. Cochran,[7] W. E. Cooper,[12] C. Cretsinger,[34] D. Cullen-Vidal,[4] M. Cummings,[14] J. P. Cussonneau,[35] D. Cutts,[4] O. I. Dahl,[19] K. De,[39] M. Demarteau,[12] R. Demina,[26] K. Denisenko,[12] N. Denisenko,[12] D. Denisov,[12] S. P. Denisov,[31] W. Dharmaratna,[13] H. T. Diehl,[12] M. Diesburg,[12] R. Dixon,[12] P. Draper,[39] J. Drinkard,[6] Y. Ducros,[35] S. Durston-Johnson,[34] D. Eartly,[12] D. Edmunds,[22] A. O. Efimov,[31] J. Ellison,[7] V. D. Elvira,[12,†] R. Engelmann,[36] S. Eno,[20] G. Eppley,[33] P. Ermolov,[23] O. V. Eroshin,[31] V. N. Evdokimov,[31] S. Fahey,[22] T. Fahland,[4] M. Fatyga,[3] M. K. Fatyga,[34] J. Featherly,[3] S. Feher,[36] D. Fein,[2] T. Ferbel,[34] G. Finocchiaro,[36] H. E. Fisk,[12] Yu. Fisyak,[23] E. Flattum,[22] G. E. Forden,[2] M. Fortner,[27] K. C. Frame,[22] P. Franzini,[10] S. Fredriksen,[37] S. Fuess,[12] E. Gallas,[39] C. S. Gao,[12,‡] T. L. Geld,[22] R. J. Genik II,[22] K. Genser,[12] C. E. Gerber,[12,§] B. Gibbard,[3] V. Glebov,[34] S. Glenn,[5] J. F. Glicenstein,[35] B. Gobbi,[28] M. Goforth,[13] A. Goldschmidt,[19] B. Gomez,[1] M. L. Good,[36] H. Gordon,[3] N. Graf,[3] P. D. Grannis,[36] D. R. Green,[12] J. Green,[27] H. Greenlee,[12] N. Grossman,[12] P. Grudberg,[19] S. Grünendahl,[34] J. A. Guida,[36] J. M. Guida,[3] W. Guryn,[3] N. J. Hadley,[20] H. Haggerty,[12] S. Hagopian,[13] V. Hagopian,[13] K. S. Hahn,[34] R. E. Hall,[6] S. Hansen,[12] J. M. Hauptman,[17] D. Hedin,[27] A. P. Heinson,[7] U. Heintz,[10] T. Heuring,[13] R. Hirosky,[13] J. D. Hobbs,[12] B. Hoeneisen,[1,‖] J. S. Hoftun,[4] Ting Hu,[36] Tong Hu,[16] J. R. Hubbard,[35] T. Huehn,[7] S. Igarashi,[12] A. S. Ito,[12] E. James,[2] J. Jaques,[29] S. A. Jerger,[22] J. Z.-Y. Jiang,[36] T. Joffe-Minor,[28] H. Johari,[26] K. Johns,[2] M. Johnson,[12] H. Johnstad,[37] A. Jonckheere,[12] M. Jones,[14] H. Jöstlein,[12] S. Y. Jun,[28] C. K. Jung,[36] S. Kahn,[3] J. S. Kang,[18] R. Kehoe,[29] M. Kelly,[29] A. Kernan,[7] L. Kerth,[19] C. L. Kim,[18] A. Klatchko,[13] B. Klima,[12] B. I. Klochkov,[31] C. Klopfenstein,[36] V. I. Klyukhin,[31] V. I. Kochetkov,[31] J. M. Kohli,[30] D. Koltick,[32] J. Kotcher,[3] J. Kourlas,[25] A. V. Kozelov,[31] E. A. Kozlovski,[31] M. R. Krishnaswamy,[38] S. Krzywdzinski,[12] S. Kunori,[20] S. Lami,[36] G. Landsberg,[36] R. E. Lanou,[4] J-F. Lebrat,[35] J. Lee-Franzini,[36] A. Leflat,[23] H. Li,[36] J. Li,[39] R. B. Li,[12,‡] Y. K. Li,[28] Q. Z. Li-Demarteau,[12] J. G. R. Lima,[8] S. L. Linn,[13] J. Linnemann,[22] R. Lipton,[12] Y. C. Liu,[28] F. Lobkowicz,[34] P. Loch,[2] S. C. Loken,[19] S. Lökös,[36] L. Lueking,[12] A. L. Lyon,[20] A. K. A. Maciel,[8] R. J. Madaras,[19] R. Madden,[13] Ph. Mangeot,[35] S. Mani,[5] I. Manning,[12] B. Mansoulié,[35] H. S. Mao,[12,‡] S. Margulies,[15] R. Markeloff,[27] L. Markosky,[2] T. Marshall,[16] M. I. Martin,[12] M. Marx,[36] B. May,[28] A. A. Mayorov,[31] R. McCarthy,[36] T. McKibben,[15] J. McKinley,[22] H. L. Melanson,[12] J. R. T. de Mello Neto,[8] X. C. Meng,[12,‡] K. W. Merritt,[12] H. Miettinen,[33] A. Milder,[2] C. Milner,[37] A. Mincer,[25] J. M. de Miranda,[8] C. S. Mishra,[12] N. Mokhov,[12] N. K. Mondal,[38] H. E. Montgomery,[12] P. Mooney,[1] M. Mudan,[25] C. Murphy,[16] C. T. Murphy,[12] F. Nang,[4] M. Narain,[12] V. S. Narasimham,[38] H. A. Neal,[21] J. P. Negret,[1] P. Nemethy,[25] D. Nešić,[4] D. Norman,[40] L. Oesch,[21] V. Oguri,[8] E. Oltman,[19] N. Oshima,[12] D. Owen,[22] P. Padley,[33] M. Pang,[17] A. Para,[12] C. H. Park,[12] R. Partridge,[4] M. Paterno,[34] A. Peryshkin,[12] M. Peters,[14] B. Pi,[22] H. Piekarz,[13] D. Pizzuto,[36] A. Pluquet,[35] V. M. Podstavkov,[31] B. G. Pope,[22] H. B. Prosper,[13] S. Protopopescu,[3] D. Pušeljić,[19] J. Qian,[21] Y.-K. Que,[12,‡] P. Z. Quintas,[12] G. Rahal-Callot,[36] R. Raja,[12] S. Rajagopalan,[36] O. Ramirez,[1] M. V. S. Rao,[38] L. Rasmussen,[36] A. L. Read,[12] S. Reucroft,[26] M. Rijssenbeek,[36] N. A. Roe,[19] J. M. R. Roldan,[1] P. Rubinov,[36] R. Ruchti,[29] S. Rusin,[23] J. Rutherfoord,[2] A. Santoro,[8] L. Sawyer,[39] R. D. Schamberger,[36] H. Schellman,[28] D. Schmid,[37] J. Sculli,[25] E. Shabalina,[23] C. Shaffer,[13] H. C. Shankar,[38] Y. Shao,[12,‡] R. K. Shivpuri,[11] M. Shupe,[2] J. B. Singh,[30] V. Sirotenko,[27] J. Skeens,[33] W. Smart,[12] A. Smith,[2] R. P. Smith,[12] R. Snihur,[28] G. R. Snow,[24] S. Snyder,[36] J. Solomon,[15] P. M. Sood,[30] M. Sosebee,[39] M. Souza,[8] A. L. Spadafora,[19] R. W. Stephens,[39] M. L. Stevenson,[19] D. Stewart,[21] F. Stocker,[37] D. A. Stoianova,[31] D. Stoker,[6] K. Streets,[25] M. Strovink,[19] A. Taketani,[12] P. Tamburello,[20] M. Tartaglia,[12] T. L. Taylor,[28] J. Teiger,[35] J. Thompson,[20] T. G. Trippe,[19] P. M. Tuts,[10] E. W. Varnes,[19] P. R. G. Virador,[19] A. A. Volkov,[31] A. P. Vorobiev,[31] H. D. Wahl,[13] D. C. Wang,[12,‡] L. Z. Wang,[12,‡] J. Warchol,[29] M. Wayne,[29] H. Weerts,[22] W. A. Wenzel,[19] A. White,[39] J. T. White,[40] J. A. Wightman,[17] J. Wilcox,[26] S. Willis,[27] S. J. Wimpenny,[7] Z. Wolf,[37] J. Womersley,[12] E. Won,[34] D. R. Wood,[12] Y. Xia,[22] D. Xiao,[13] R. P. Xie,[12,‡] H. Xu,[4] R. Yamada,[12] P. Yamin,[3] C. Yanagisawa,[36] J. Yang,[25] M.-J. Yang,[12] T. Yasuda,[26] C. Yoshikawa,[14] S. Youssef,[13]

 0031-9007/95/74(13)/2422(5)$06.00

J. Yu,[34] C. Zeitnitz,[2] D. Zhang,[12,‡] Y. Zhang,[12,‡] Z. Zhang,[36] Y. H. Zhou,[12,‡] Q. Zhu,[25] Y. S. Zhu,[12,‡] D. Zieminska,[16] A. Zieminski,[16] A. Zinchenko,[17] and A. Zylberstejn[35]

(D0 Collaboration)

[1]*Universidad de los Andes, Bogota, Colombia*
[2]*University of Arizona, Tucson, Arizona 85721*
[3]*Brookhaven National Laboratory, Upton, New York 11973*
[4]*Brown University, Providence, Rhode Island 02912*
[5]*University of California, Davis, California 95616*
[6]*University of California, Irvine, California 92717*
[7]*University of California, Riverside, California 92521*
[8]*LAFEX, Centro Brasileiro de Pesquisas Físicas, Rio de Janeiro, Brazil*
[9]*Centro de Investigacion y de Estudios Avanzados, Mexico City, Mexico*
[10]*Columbia University, New York, New York 10027*
[11]*Delhi University, Delhi, India 110007*
[12]*Fermi National Accelerator Laboratory, Batavia, Illinois 60510*
[13]*Florida State University, Tallahassee, Florida 32306*
[14]*University of Hawaii, Honolulu, Hawaii 96822*
[15]*University of Illinois, Chicago, Illinois 60680*
[16]*Indiana University, Bloomington, Indiana 47405*
[17]*Iowa State University, Ames, Iowa 50011*
[18]*Korea University, Seoul, Korea*
[19]*Lawrence Berkeley Laboratory, Berkeley, California 94720*
[20]*University of Maryland, College Park, Maryland 20742*
[21]*University of Michigan, Ann Arbor, Michigan 48109*
[22]*Michigan State University, East Lansing, Michigan 48824*
[23]*Moscow State University, Moscow, Russia*
[24]*University of Nebraska, Lincoln, Nebraska 68588*
[25]*New York University, New York, New York 10003*
[26]*Northeastern University, Boston, Massachusetts 02115*
[27]*Northern Illinois University, DeKalb, Illinois 60115*
[28]*Northwestern University, Evanston, Illinois 60208*
[29]*University of Notre Dame, Notre Dame, Indiana 46556*
[30]*University of Panjab, Chandigarh 16-00-14, India*
[31]*Institute for High Energy Physics, 142-284 Protvino, Russia*
[32]*Purdue University, West Lafayette, Indiana 47907*
[33]*Rice University, Houston, Texas 77251*
[34]*University of Rochester, Rochester, New York 14627*
[35]*Commissariat à l'Energie Atomique, DAPNIA/Service de Physique des Particules, Centre d'Etudes de Saclay, Saclay, France*
[36]*State University of New York, Stony Brook, New York 11794*
[37]*Superconducting Super Collider Laboratory, Dallas, Texas 75237*
[38]*Tata Institute of Fundamental Research, Colaba, Bombay 400005, India*
[39]*University of Texas, Arlington, Texas 76019*
[40]*Texas A&M University, College Station, Texas 77843*

(Received 7 November 1994)

We present new results on the search for the top quark in $p\bar{p}$ collisions at $\sqrt{s} = 1.8$ TeV with an integrated luminosity of 13.5 ± 1.6 pb^{-1}. We have considered $t\bar{t}$ production in the standard model using electron and muon dilepton decay channels ($t\bar{t} \to e\mu$ + jets, ee + jets, and $\mu\mu$ + jets) and single-lepton decay channels ($t\bar{t} \to e$ + jets and μ + jets) with and without tagging of b quark jets. From all channels we have nine events with an expected background of 3.8 ± 0.9. If we assume that the excess is due to $t\bar{t}$ production, and assume a top mass of 180 GeV/c^2, we obtain a cross section of 8.2 ± 5.1 pb.

PACS numbers: 14.65.Ha, 13.85.Qk, 13.85.Rm

In the standard model (SM), the top quark is the weak isospin partner of the b quark. Precision electroweak measurements indirectly constrain the SM top quark mass to be $178 \pm 11^{+18}_{-19}$ GeV/c^2 [1]. The D0 Collaboration recently published a lower limit on the mass of the top quark of 131 GeV/c^2, at a confidence level of 95% [2]. The CDF Collaboration has presented evidence for top quark production of mass $174 \pm 10^{+13}_{-12}$ GeV/c^2 with a cross section of $13.9^{+6.1}_{-4.8}$ pb [3]. The present analysis, which is based on the same data sample as Ref. [2], includes three additional top quark decay channels, reoptimizes the event selection criteria for higher mass top, and

provides a background-subtracted estimate of the top production cross section [4].

We assume that the top quark is pair produced and decays according to the minimal SM (i.e., $t\bar{t} \to W^+W^- b\bar{b}$), and subsequently the W decays into leptons ($W \to \ell\bar{\nu}$, where $\ell = e, \mu$, or τ) or quarks. We searched for the following distinct decay channels: (a) $t\bar{t} \to \ell_1\bar{\ell}_2\bar{\nu}_1\nu_2 b\bar{b}$, the dilepton channels, with branching fractions 2/81 for $e\mu$ + jets and 1/81 each for ee + jets and $\mu\mu$ + jets, and (b) $t\bar{t} \to \ell\bar{\nu}q\bar{q}' b\bar{b}$, the single-lepton channels e + jets and μ + jets, each with a branching reaction of 12/81. The latter were further subdivided into b-tagged and untagged channels according to whether or not a soft muon was observed. We denote the soft-μ-tagged channels by e + jets/μ and μ + jets/μ. The probability that at least one of the two b quarks in a $t\bar{t}$ event will decay to a muon, either directly or through a cascade ($b \to c \to \mu$), is approximately 40% [5].

The D0 detector and data collection systems are described in Ref. [6]. The basic elements of the trigger and reconstruction algorithms for jets, electrons, muons, and neutrinos are given in Ref. [2].

Muons were detected and momentum analyzed using an iron toroid spectrometer outside of a uranium-liquid argon calorimeter and a nonmagnetic central tracking system inside the calorimeter. Muons were identified by their ability to penetrate the calorimeter and the spectrometer magnet yoke. Two distinct types of muons were defined. "High-p_T" muons, which are predominantly from gauge boson decay, were required to be isolated from jet axes by distance $\Delta\mathcal{R} > 0.5$ in η-ϕ space [η = pseudorapidity = $\tanh^{-1}(\cos\theta)$; θ, ϕ = polar, azimuthal angle], and to have transverse momentum $p_T > 12$ GeV/c. "Soft" muons, which are primarily from b, c, or π/K decay, were required to be within distance $\Delta\mathcal{R} < 0.5$ of any jet axis or, alternatively, to have a p_T less than the minimum of a high-p_T muon. The minimum p_T for soft muons was 4 GeV/c and the maximum η for both kinds of muons was 1.7.

Electrons were identified by their longitudinal and transverse shower profile in the calorimeter, and were required to have a matching track in the central tracking chambers. The background from photon conversions was reduced relative to that in Ref. [2] by the imposition of an ionization (dE/dx) criterion on the chamber track. Electrons were required to have $|\eta| < 2.5$ and transverse energy $E_T > 15$ GeV.

Jets were reconstructed using a cone algorithm of radius $\mathcal{R} = 0.5$ with a minimum E_T of 8 GeV. The minimum E_T for jets to be included in the top analysis was either 15 or 20 GeV (see Table I).

The presence of neutrinos in the final state was inferred from missing transverse energy ($\not\!\!E_T$). The calorimeter-only $\not\!\!E_T$ ($\not\!\!E_T^{\rm cal}$) was determined from energy deposition in the calorimeter for $|\eta| < 4.5$. The total $\not\!\!E_T$ was determined by correcting $\not\!\!E_T^{\rm cal}$ for the measured p_T of detected muons.

TABLE I. Selection criteria for the seven top channels.

$e\mu$ + jets	$\geq$1 electron ($E_T > 15$ GeV, $\|\eta\| < 2.5$) $\geq$1 high-p_T muon ($p_T > 12$ GeV/c, $\|\eta\| < 1.7$) $\Delta\mathcal{R}(e,\mu) > 0.25$ $\geq$2 jets ($E_T > 15$ GeV, $\|\eta\| < 2.5$) $\not\!\!E_T^{\rm cal} > 20$ GeV, $\not\!\!E_T > 10$ GeV
ee + jets	$\geq$2 electrons ($E_T > 20$ GeV, $\|\eta\| < 2.5$) $\geq$2 jets ($E_T > 15$ GeV, $\|\eta\| < 2.5$) $\not\!\!E_T^{\rm cal} > 25$ GeV $\not\!\!E_T^{\rm cal} > 40$ GeV if $\|m_{ee} - m_Z\| < 12$ GeV
$\mu\mu$ + jets	$\geq$2 high-p_T muons ($p_T > 15$ GeV/c, $\|\eta\| < 1.1$) $\geq$2 jets ($E_T > 15$ GeV, $\|\eta\| < 2.5$) $m_{\mu\mu} > 10$ GeV/c^2 $\Delta\phi^{\mu\mu} < 140°$ if $\not\!\!E_T < 40$ GeV $\Delta\phi(\not\!\!E_T^{\rm cal}, p_T^{\mu\mu}) > 30°$
e + jets	1 electron ($E_T > 20$ GeV, $\|\eta\| < 2.0$) No soft muons $\geq$4 jets ($E_T > 15$ GeV, $\|\eta\| < 2.0$) $\not\!\!E_T^{\rm cal} > 25$ GeV $\mathcal{A} > 0.05$, $H_T > 140$ GeV
μ + jets	1 high-p_T muon ($p_T > 15$ GeV/c, $\|\eta\| < 1.7$) No soft muons $\geq$4 jets ($E_T > 15$ GeV, $\|\eta\| < 2.0$) $\not\!\!E_T^{\rm cal} > 20$ GeV, $\not\!\!E_T > 20$ GeV $\mathcal{A} > 0.05$, $H_T > 140$ GeV
e + jets/μ	1 electron ($E_T > 20$ GeV, $\|\eta\| < 2.0$) $\geq$1 soft muon ($p_T > 4$ GeV/c, $\|\eta\| < 1.7$) $\geq$3 jets ($E_T > 20$ GeV, $\|\eta\| < 2.0$) $\not\!\!E_T^{\rm cal} > 20$ GeV $\not\!\!E_T^{\rm cal} > 35$ GeV if $\Delta\phi(\not\!\!E_T^{\rm cal}, \mu) < 25°$
μ + jets/μ	1 high-p_T muon ($p_T > 15$ GeV/c, $\|\eta\| < 1.7$) $\geq$1 soft muon ($p_T > 4$ GeV/c, $\|\eta\| < 1.7$) $\geq$3 jets ($E_T > 20$ GeV, $\|\eta\| < 2.0$) $\not\!\!E_T^{\rm cal} > 20$ GeV, $\not\!\!E_T > 20$ GeV For highest p_T muon: $\Delta\phi(\not\!\!E_T, \mu) < 170°$ and $\|\Delta\phi(\not\!\!E_T, \mu) - 90°\|/90° < \not\!\!E_T/(45$ GeV)

The acceptance for $t\bar{t}$ events was calculated for several top masses using the ISAJET event generator [7] and a detector simulation based on the GEANT program [8].

Physics backgrounds (those having the same final state particles as the signal) were estimated by Monte Carlo simulation or from a combination of Monte Carlo and data. The instrumental background from jets misidentified as electrons was estimated entirely from data using the measured jet misidentification probability (typically 2×10^{-4}). Other backgrounds for muons (e.g., hadronic punchthrough and cosmic rays) were found to be negligible for the signatures in question.

The signature for dilepton channels was defined as having two high-p_T isolated leptons, two jets, and large $\not\!\!E_T$. The selection criteria are summarized in Table I.

Physics backgrounds to the dilepton channels stem mainly from Z and continuum Drell-Yan production ($Z, \gamma^* \to ee, \mu\mu$, and $\tau\tau$), vector boson pairs (WW, WZ),

TABLE II. Efficiency × branching fraction ($\varepsilon \times \mathcal{B}$) and the expected number of events ($\langle N \rangle$) in the seven channels, based on the central theoretical $t\bar{t}$ production cross section of Ref. [12], for four top masses. Also given are the expected backgrounds, integrated luminosity, and the number of observed events in each channel.

m_t(GeV/c^2)	$e\mu$ + jets	ee + jets	$\mu\mu$ + jets	e + jets	μ + jets	e + jets/μ	μ + jets/μ	All
$\varepsilon \times \mathcal{B}$ (%)	0.31 ± 0.04	0.18 ± 0.02	0.15 ± 0.02	1.1 ± 0.3	0.8 ± 0.2	0.6 ± 0.2	0.4 ± 0.1	
140 $\langle N \rangle$	0.71 ± 0.12	0.41 ± 0.07	0.25 ± 0.04	2.5 ± 0.7	1.3 ± 0.4	1.4 ± 0.5	0.7 ± 0.2	7.2 ± 1.3
$\varepsilon \times \mathcal{B}$ (%)	0.36 ± 0.05	0.20 ± 0.03	0.15 ± 0.02	1.5 ± 0.4	1.1 ± 0.3	0.9 ± 0.2	0.5 ± 0.1	
160 $\langle N \rangle$	0.40 ± 0.07	0.22 ± 0.04	0.12 ± 0.02	1.7 ± 0.5	0.9 ± 0.3	1.0 ± 0.3	0.4 ± 0.1	4.7 ± 0.8
$\varepsilon \times \mathcal{B}$ (%)	0.39 ± 0.05	0.21 ± 0.03	0.14 ± 0.02	1.6 ± 0.4	1.1 ± 0.3	1.1 ± 0.2	0.7 ± 0.1	
180 $\langle N \rangle$	0.22 ± 0.04	0.12 ± 0.02	0.06 ± 0.01	0.9 ± 0.3	0.5 ± 0.1	0.6 ± 0.1	0.3 ± 0.1	2.7 ± 0.4
$\varepsilon \times \mathcal{B}$ (%)	0.40 ± 0.05	0.30 ± 0.04	0.14 ± 0.02	1.8 ± 0.4	1.3 ± 0.3	1.4 ± 0.1	0.8 ± 0.2	
200 $\langle N \rangle$	0.12 ± 0.02	0.09 ± 0.02	0.03 ± 0.01	0.5 ± 0.1	0.3 ± 0.1	0.4 ± 0.1	0.2 ± 0.1	1.7 ± 0.3
Background	0.27 ± 0.06	0.16 ± 0.07	0.33 ± 0.06	1.3 ± 0.7	0.7 ± 0.5	0.6 ± 0.2	0.4 ± 0.1	3.8 ± 0.9
$\int \mathcal{L} dt$ (pb^{-1})	13.5 ± 1.6	13.5 ± 1.6	9.8 ± 1.2	13.5 ± 1.6	9.8 ± 1.2	13.5 ± 1.6	9.8 ± 1.2	
Data	1	0	0	2	2	2	2	9

and heavy flavor ($b\bar{b}$ and $c\bar{c}$) jet production. The $e\mu$ + jets and ee + jets channels have additional backgrounds from jets misidentified as electrons. The background estimates obtained with the new selection criteria are more than a factor of 2 lower than those of Ref. [2], whereas the acceptance for the $t\bar{t}$ signal in the high mass region ($m_t > 130$ GeV/c^2) is similar. Table II shows the acceptances and the expected number of $t\bar{t}$ events for four values of the top mass, the total expected background, and the number of observed events. The $e\mu$ event that passes all selections was discussed in Ref. [2].

The signature of the single-lepton channels was defined as having one high-p_T lepton, large $\not\!\!E_T$, and a minimum of three jets (with soft μ tag) or four jets (without tag). For the untagged channels, additional background rejection was achieved through event shape criteria based on the aplanarity of the jets in the laboratory frame, $\mathcal{A}$ [9], and on the scalar sum of the E_T's of the jets, which we call H_T. The criteria used for selecting the single-lepton channels are shown in Table I. Only the jets that passed the criteria of Table I were used in calculating $\mathcal{A}$ and H_T.

The main backgrounds to the single-lepton $t\bar{t}$ channels were from W + jets, Z + jets (for μ + jets/μ, and multijet events where one jet was misidentified as an isolated lepton. The latter do not normally have large $\not\!\!E_T$. We estimated the multijet background directly from data, based on the joint probability of multijet events having large $\not\!\!E_T$ and a jet being misidentified as a lepton.

Figure 1 shows the number of Z- and multijet-background-subtracted W + jets events, for electrons and muons combined, as a function of the minimum jet multiplicity, with and without soft μ tag. The $\not\!\!E_T$ and jet E_T criteria were those of Table I for the untagged and tagged analyses respectively. Also shown is a prediction of the number of soft-μ-tagged W + jets events derived from the number of untagged events folded with tagging rates obtained from multijet data. The multijet tagging probability was observed to increase linearly with the number of jets, being approximately 1.5% per event for events with three or more jets, and 2.0% per event for events with four or more jets. In contrast, the soft-μ-tagging probability for top quark events is calculated by Monte Carlo simulation to be about 20% per event. An admixture of a top signal in W + jets events could appear in high jet multiplicities (three or four jets) as excess untagged or tagged events. In the absence of top, the number of W + jets events is expected to decrease exponentially as a function of the jet multiplicity [10]. The observed number of tagged events is higher than the number expected from background, but the significance of the excess is low.

The untagged single-lepton analysis made use of the distribution of events in the $\mathcal{A}$-H_T plane. Figure 2 shows scatter plots of $\mathcal{A}$ vs H_T for (a) expected multijet background, (b) expected W + 4 jet background, (c) 180 GeV/c^2 top, and (d) the observed distribution for untagged lepton + 4 jet events. The multijet background was calculated from data by the method described above. The points in Fig. 2(a) are data points with a loosened electron requirement, excluding real electrons. The prediction for the untagged W + 4 jet background [Fig. 2(b)] was calculated using the VECBOS Monte Carlo

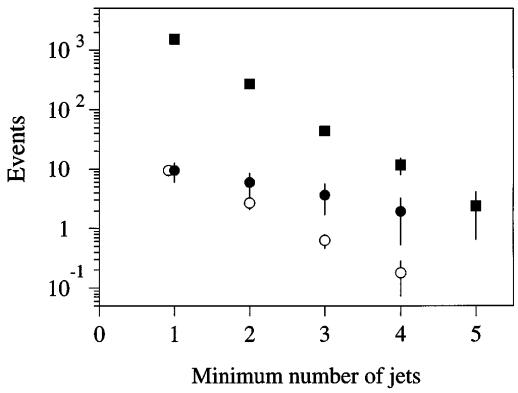

FIG. 1. The observed number of untagged (solid squares) and soft-μ-tagged (solid circles) W + jets events, after Z and multijet background subtraction, and the number of soft-μ-tagged events expected in the absence of top (open circles), as a function of the minimum number of jets.

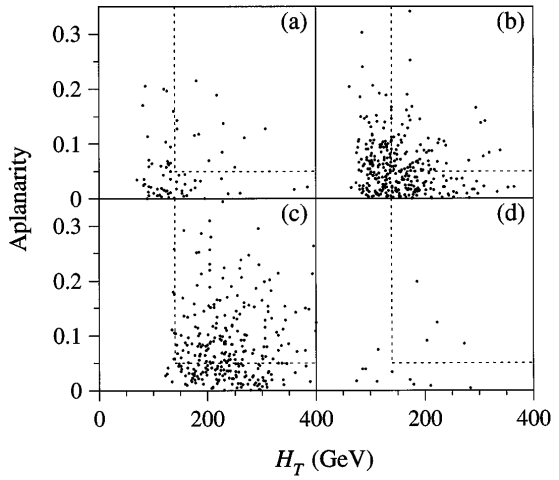

FIG. 2. $\mathcal{A}$ vs H_T for single-lepton events for (a) multijet background from data (effective luminosity = 60 × data luminosity), (b) background from W + 4 jet VECBOS Monte Carlo simulation (580 pb^{-1}), (c) 180 GeV/c^2 top ISAJET Monte Carlo simulation (2200 pb^{-1}), and (d) data (13.5 pb^{-1}). The dotted lines represent the event shape cuts used in the analysis.

program [11]. The absolute normalization of the latter is not well known due to theoretical uncertainties. We normalized the W background directly from the data by two independent methods. The first method was exponential extrapolation from one and two jets to four jets. The second method was to fit the observed distribution of events in the entire $\mathcal{A}$-H_T plane [Fig. 2(d)] to a linear combination of signal and background [Figs. 2(a)–2(c)]. The backgrounds and errors determined by the two methods agree (1.9 ± 0.7 vs 2.1 ± 0.8). Our final background estimate is the average of the two methods.

Table II summarizes the results for all seven channels. Adding all seven channels together, there are nine observed events with an expected background of 3.8 ± 0.9 events. In the absence of top, we calculate the probability of an upward fluctuation of the background to nine or more events to be 2.7%.

If we assume that the observed excess is due to $t\bar{t}$ production, we can calculate the top cross section according to the equation $\sigma_{t\bar{t}} = \sum_{i=1}^{7}(N_i - B_i)/\sum_{i=1}^{7}\varepsilon_i \mathcal{B}_i L_i$, where N_i is the number of observed events for decay channel i, B_i is the expected background, ε_i is the detection efficiency for a particular top mass, $\mathcal{B}_i$ is the branching fraction, and L_i is the integrated luminosity. The results are plotted in Fig. 3. For the 180 GeV/c^2 (160 GeV/c^2) top mass hypothesis, the top production cross section is 8.2 ± 5.1 pb (9.2 ± 5.7 pb). This cross section is consistent with theoretical expectations for the SM top quark [12]. Our measurement, although consistent with the CDF result [3] and of comparable sensitivity, does not demonstrate the existence of the top quark.

We thank the Fermilab Accelerator, Computing, and Research Divisions, and the support staffs at the collaborating institutions for their contributions to the success of this work. We also acknowledge the support of the U.S. Department of Energy, the U.S. National Science Foundation, the Commissariat à L'Energie Atomique in France, the Ministry for Atomic Energy in Russia, CNPq in Brazil, the Departments of Atomic Energy and Science and Education in India, Colciencias in Colombia, CONACyT in Mexico, and the Ministry of Education, Research Foundation and KOSEF in Korea.

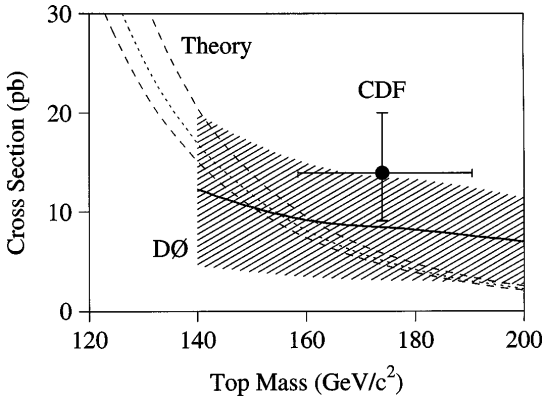

FIG. 3. D0 measured $t\bar{t}$ production cross section (solid line, shaded band = one standard deviation error) as a function of top mass hypothesis. Also shown are central (dotted line), high, and low (dashed lines) theoretical cross section curves [12], and the CDF measurement [3].

*Visitor from LAL, Orsay, France.
†Visitor from CONICET, Argentina.
‡Visitor from IHEP, Beijing, China.
§Visitor from Universidad de Buenos Aires, Argentina.
‖Visitor from Univ. San Francisco de Quito, Ecuador.

[1] D. Schaile, in Proceedings of the 27th International Conference on High Energy Physics, Glasgow, 1994 (Report No. CERN-PPE/94-162).
[2] D0 Collaboration, S. Abachi *et al.*, Phys. Rev. Lett. **72**, 2138 (1994).
[3] CDF Collaboration, F. Abe *et al.*, Phys. Rev. D **50**, 2966 (1994); Phys. Rev. Lett. **73**, 225 (1994).
[4] The integrated luminosity used in the present analysis has been lowered by 12% relative to Ref. [2] due to a change in the world average measured $p\bar{p}$ total cross section as described in N. Amos *et al.*, Fermilab Report No. FERMILAB-TM-1911, 1994 (unpublished).
[5] Particle Data Group, L. Montanet *et al.*, Phys. Rev. D **50**, 1173 (1994).
[6] D0 Collaboration, S. Abachi *et al.*, Nucl. Instrum. Methods Phys. Res., Sect. A **338**, 185 (1994).
[7] F. Paige and S. Protopopescu, BNL Report No. BNL38034, 1986 (unpublished), release v 6.49.
[8] F. Carminati *et al.*, "GEANT Users Guide," CERN Program Library, 1991 (unpublished).
[9] V. Barger, J. Ohnemus, and R. J. N. Phillips, Phys. Rev. D **48**, 3953 (1993).
[10] F. Berends, H. Kuijf, B. Tausk, and W. Giele, Nucl. Phys. **B357**, 32 (1991).
[11] W. Giele, E. Glover, and D. Kosower, Nucl. Phys. **B403**, 633 (1993).
[12] E. Laenen, J. Smith, and W. van Neerven, Phys. Lett. B **321**, 254 (1994).